

On the Simultaneous Conjugate Match of N -Port Networks

Sergio Colangeli¹, Antonio Serino¹, Walter Ciccognani¹, Patrick E. Longhi¹, *Member, IEEE*,
and Ernesto Limiti¹, *Senior Member, IEEE*

Abstract—Some advancements are proposed to the theory of simultaneous conjugate match (SCM) of N -ports. It is shown that, if a network qualifies for geometrical unconditional stability (g -US), then it can be matched simultaneously at all ports. The proof serves as the basis for constructing an iterative algorithm (AlgG) which is guaranteed to converge to the SCM condition for all N -ports exhibiting g -US. In addition to the main results above mentioned, two more iterative algorithms are presented (AlgS and AlgA), which are conjectured to work for all networks satisfying g -US. AlgS can be shown to converge globally for $N = 2$ and AlgA to converge locally for all N . Besides their theoretical interest, these results find a natural application in the matching of passive networks, and in particular of N -element phased arrays. However, they can be applied to any (i.e., also active) N -port as long as this is known to exhibit g -US.

Index Terms—Linear networks, simultaneous conjugate match (SCM), unconditional stability.

I. INTRODUCTION

HIGH-FREQUENCY circuits are typically required to be matched to a common impedance (usually, $Z_0 = 50 \Omega$). In this way, at least as a first approximation, they can be directly connected to build more complex systems without the need for taking into account mutual loading effects. In the case of purely passive components (filters, combiners, hybrids), Z_0 -matching is generally built in the design equations themselves. On the other hand, transistor-based components (in particular, amplifiers) are matched to Z_0 by means of ad hoc two-ports called “matching networks.”

In general, cascading a matching network to one port of a circuit affects the matching level at all other ports too, in a complicated manner. Fortunately, if the circuit under analysis is a two-port (which is by far the most common case), closed-form expressions are available for the terminations realizing a simultaneous conjugate match (SCM), as well as the conditions under which those terminations are passive. Passivity of the terminations is a key feature, since it allows using lossless, reciprocal matching networks to transform the external standard impedance (which is passive) to the computed SCM terminations. It turns out that (strictly) passive values of the SCM terminations are possible at a given frequency

if and only if the two-port has a stability factor K [1], [2] greater than unity (see Appendix). Notice that all unconditionally stable (us) two-ports satisfy this condition (asymptotic stability is considered in this article when not specified otherwise).

As to N -ports with $N > 2$, little information is available in the literature, mostly limited to lossless networks (see [3] and references therein). One noteworthy result from the theory of linear time-invariant networks states that no such three-port can be realized which is at the same time lossless, reciprocal and matched at all ports [4]. However, the problem of simultaneous matching of N -ports does not seem to have been addressed for general networks (i.e., including the active ones and for arbitrary N).

In this article, the main result will be shown first: namely, Section IV proves that, if an N -port network (with arbitrary N) is geometrically us (g - us , where the terminology follows from [5], [6]), then SCM can always be attained by iteratively improving the driving-point reflectances at all ports. Further, Section V shows how to translate the iterative scheme into a numerical algorithm (AlgG).

In addition to the main results above, two additional algorithms are presented in Section VI, namely AlgS and AlgA. Unlike AlgG, which is integral to the core of this contribution, AlgS and AlgA are presented as a starting point for further developments. The possibility of brute optimization is also commented on in Section VI. It is important to stress that the advantage of AlgG lies in the guarantee that, under g -US, it converges to the SCM condition. On the contrary, with general-purpose optimizers there is no mathematical guarantee that the global optimum is actually found, since the optimization problem is not convex. On top of that, the link between g -US and matching for arbitrary N would not have emerged if lazy reliance on brute optimization had not been questioned.

Examples of applications of the presented theory to actual networks are proposed in Section VII. First, a circuit example is worked out in full, from the design of ideal matching networks to a full-fledged electromagnetic (EM) simulation, to realization and measurement. Notice that the presented results can be directly applied to the problem of simultaneously matching phased arrays composed by an arbitrary number of elements [7]: thus, two examples represented by a ten-element and a three-element array are provided. Finally, a paraphase amplifier is selected to show the application of the presented results to an active circuit.

Manuscript received 8 January 2024; revised 9 February 2024; accepted 27 February 2024. (Corresponding author: Sergio Colangeli.)

The authors are with the Department of Electronics Engineering, University of Rome Tor Vergata, 00133 Rome, Italy (e-mail: colangeli@ing.uniroma2.it).

Color versions of one or more figures in this article are available at <https://doi.org/10.1109/TMTT.2024.3372332>.

Digital Object Identifier 10.1109/TMTT.2024.3372332

TABLE I
DEFINITION OF MAIN N -PORT CLASSES IN SECTION II

Attribute	Defining property	Further reading
g - us at f_0	$\det[\mathbf{L}\mathbf{S} - \mathbf{1}]$ is devoid of positive zeros and multiple imaginary zeros for any non-active termination set \mathbf{L} at frequency f_0 (maps non-active terminations at ports $j \neq i$ into non-active reflectances at port i)	[5], [6]
strictly g - us at f_0	$\det[\mathbf{L}\mathbf{S} - \mathbf{1}]$ is devoid of nonnegative zeros and multiple imaginary zeros for any non-active set of termination set \mathbf{L} at frequency f_0 (maps non-active terminations at ports $j \neq i$ into strictly passive reflectances at port i)	[5], [6]
us	g - us for all f_0	[1], [8]
strictly us	strictly g - us for all f_0	[1], [8]
passive at f_0	$\mathbf{1} - \mathbf{S}^H\mathbf{S}$ is positive semi-definite at frequency f_0	[9]
strictly passive at f_0	$\mathbf{1} - \mathbf{S}^H\mathbf{S}$ is positive definite at frequency f_0	[9]

Note: superscript H denotes the Hermitian transpose operator.

II. TERMINOLOGY AND GENERAL FRAMEWORK

Given a network realized by connecting N terminations and an N -port linear circuit (possibly representing the linearized solution of a nonlinear one), the N -port is said to be unconditionally stable (us) if and only if the network functions of the overall connection cannot exhibit unstable poles irrespective of the terminations, as long as these are not active. When dealing with passive circuits, this definition includes the reactive ones. However, when considering active circuits, it is more useful to restrict the focus to asymptotic stability, which demands strictly stable poles under all possible choices of passive terminations [8].

If a linear circuit is us , then at any given frequency f_0 it necessarily maps passive terminations at $N - 1$ ports into a passive driving-point impedance at the remaining port. For reasons of convenience and technical correctness, an N -port satisfying this less restrictive condition at f_0 is here referred to as geometrically us (g - us) [5], [6]. For future use, it is convenient to reappraise here a recent result [5] stating that the scattering parameters S_{ij} of a strictly g - us N -port satisfy the following condition:

$$\sum_{j=1}^N |S_{ij}S_{ji}| < 1 \quad \forall i. \quad (1)$$

(Notice that there is a material error in [5, Sec. III-D], whereby $\rho_s(\mathbf{d}) = \infty$ and $\rho_s(\mathbf{d}) < \infty$ are mistakenly used in place of $\mathbf{d} = \mathbf{0}$ and $\mathbf{d} \neq \mathbf{0}$, respectively.)

The relations among the classes of linear networks which are of interest for the purposes of the present contribution are represented graphically in Fig. 1, whereas technical definitions are summarized in Table I. In particular, the class of networks for which the main result holds true is that of strictly g - us N -ports (grayed area in the graph). Notice that this class includes the passive N -ports which are strictly lossy at f_0 , but not the reactive (lossless) ones.

Thus, from a theoretical standpoint, passivity is not a necessary requirement for applying the presented result. However, from a practical perspective, the most interesting examples of g - us N -ports, when $N > 2$, are arguably passive, as discussed at the beginning of Section VII. In this regard it is worth

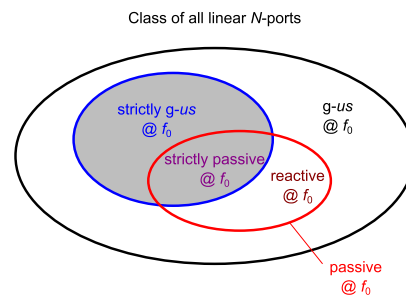


Fig. 1. Relation among the different classes of linear N -ports mentioned in Section II.

pointing out that, if the considered N -port is strictly passive (a condition very easy to check [9]), then it is guaranteed to be strictly g - us without further verifications. On the other hand, checking whether an active N -port is g - us or not is rather difficult when $N > 2$ [6], [10], [11].

III. BASIC NETWORK OPERATIONS

A. Lossless Matching Network

The iterative algorithms presented in this contribution make extensive use of two-port matching networks, placed in cascade to the ports of the N -port circuit to be iteratively matched. Under the assumptions that these matching networks are reciprocal and lossless and that they transform the zero reflectance at the external port (left-hand side) into Γ at the connection port (right-hand side), the most general form of their scattering matrix is as follows:

$$\mathbf{F} = \begin{bmatrix} -\Gamma^* e^{j2\phi_a} & \sqrt{1 - |\Gamma|^2} e^{j\phi_a} \\ \sqrt{1 - |\Gamma|^2} e^{j\phi_a} & \Gamma \end{bmatrix} \quad (2)$$

where $|\Gamma| < 1$ and ϕ_a is an arbitrary phase. For simplicity, ϕ_a can be considered equal to zero for a basic matching network (in fact, we will assume $\phi_a = 0$ outside this Section). A nonzero ϕ_a would correspond to cascading a length of matched lossless transmission line ahead of the basic configuration. As to Γ , it is set equal to $d\Gamma_{L,i}$ in Section IV and to S_{ii}^* elsewhere.

Notice that $|\Gamma| = 1$ would also technically result in a lossless two-port, but one exhibiting a transmission zero.

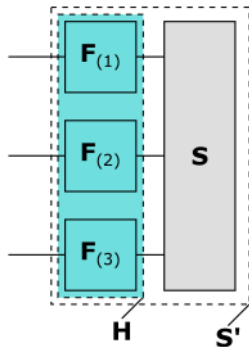


Fig. 2. Construction used in Section IV, exemplified in the case $N = 3$. The matrix definitions here shown are used for both AlgG and AlgA and are consistent with Sections III-A and III-B.

We refer to this kind of network as a “degenerate” lossless two-port.

B. Network Embedding

Given two scattering matrices, \mathbf{S} of size $N \times N$ and \mathbf{H} of size $2N \times 2N$, it is possible to embed \mathbf{S} into \mathbf{H} to obtain a new matrix \mathbf{S}' of size $N \times N$. In particular, splitting \mathbf{H} into four $N \times N$ sub-blocks yields

$$\mathbf{H} = \begin{bmatrix} \mathbf{A} & \mathbf{B} \\ \mathbf{C} & \mathbf{D} \end{bmatrix} \quad (3)$$

$$\mathbf{S}' = \mathbf{A} + \mathbf{B} \cdot (\mathbf{S}^{-1} - \mathbf{D})^{-1} \cdot \mathbf{C}. \quad (4)$$

In the particular case that \mathbf{H} is made up of N quadrupoles with matrices $\mathbf{F}_{(i)}$ (each associated with a port of \mathbf{S} , as shown in Fig. 2), then \mathbf{A} , \mathbf{B} , \mathbf{C} and \mathbf{D} are diagonal matrices, whose i -th diagonal elements correspond with the (1, 1), (1, 2), (2, 1) and (2, 2) elements, respectively, of $\mathbf{F}_{(i)}$, i.e.,

$$\mathbf{A} = \text{diag}([F_{(1),11} \quad \cdots \quad F_{(N),11}]) \quad (5)$$

$$\mathbf{B} = \text{diag}([F_{(1),12} \quad \cdots \quad F_{(N),12}]) \quad (6)$$

$$\mathbf{C} = \text{diag}([F_{(1),21} \quad \cdots \quad F_{(N),21}]) \quad (7)$$

$$\mathbf{D} = \text{diag}([F_{(1),22} \quad \cdots \quad F_{(N),22}]). \quad (8)$$

Notice that, if \mathbf{S} is strictly g - us and all $\mathbf{F}_{(i)}$ are non-degenerate lossless two-ports, then \mathbf{S}' is strictly g - us too. On the other hand, if at least one $\mathbf{F}_{(i)}$ is a degenerate lossless two-port, \mathbf{S}' becomes marginally g - us .

IV. ATTAINABILITY OF THE SCM CONDITION FOR G - us N -PORTS

Consider a g - us N -port with scattering matrix \mathbf{S} at f_0 and terminated in matched loads at all ports—i.e., loads with zero reflectance, given the relevant reference impedances. The latter are assumed to be lossy but need not be strictly resistive, as long as Kurokawa’s “power-wave” convention is adopted [9].

Now choose arbitrary perturbations of the (matched) loads, $d\Gamma_1, d\Gamma_2, \dots, d\Gamma_N$. Each of these can be decomposed as a variation in magnitude ($d\rho_i$) and a rotation ($e^{j\phi_i}$). With reference to Fig. 2 and in accordance with Sections III-A

and III-B, define

$$\mathbf{A} = \begin{bmatrix} -d\Gamma_1^* & & & \\ & \ddots & & \\ & & & -d\Gamma_N^* \end{bmatrix} \quad (9)$$

$$\mathbf{B} = \mathbf{C} = \begin{bmatrix} \sqrt{1 - |d\Gamma_1|^2} & & & \\ & \ddots & & \\ & & & \sqrt{1 - |d\Gamma_N|^2} \end{bmatrix} \quad (10)$$

$$\mathbf{D} = \begin{bmatrix} d\Gamma_1 & & & \\ & \ddots & & \\ & & & d\Gamma_N \end{bmatrix} \quad (11)$$

realizing a reactive embedding of the original network. The scattering matrix \mathbf{S}' obtained after such an embedding is a perturbation of \mathbf{S} , as follows:

$$\mathbf{S}' = \mathbf{A} + \mathbf{B} \cdot (\mathbf{S}^{-1} - \mathbf{D})^{-1} \cdot \mathbf{C} \quad (12)$$

$$= \mathbf{A} - \mathbf{B}\mathbf{S}\mathbf{M}^{-1}\mathbf{C} \quad (13)$$

$$\approx \mathbf{A} - \mathbf{S}\mathbf{M}^{-1} \quad (14)$$

where

$$\mathbf{M} = \mathbf{D}\mathbf{S} - \mathbf{1} \quad (15)$$

and (14) follows from (13) as a first-order approximation in the Γ_i terms (thus, $\mathbf{B} = \mathbf{C} \approx \mathbf{1}$). Notice that matrix \mathbf{M} is always invertible if the network is g - us [6], [10], [12], [13], so that \mathbf{S}' is certainly finite.

Since \mathbf{M} can be inverted, its inverse too can be linearized for small Γ_i terms, resulting in $\mathbf{M}^{-1} \approx -(\mathbf{1} + \mathbf{D}\mathbf{S})$. Plugging this into (14) and expanding yields

$$\mathbf{S}' \approx \mathbf{S} + \mathbf{A} + \mathbf{S}\mathbf{D}\mathbf{S}. \quad (16)$$

Then, extracting the diagonal scattering parameters and approximating again to the first order yields

$$\begin{bmatrix} S'_{11} \\ \vdots \\ S'_{NN} \end{bmatrix} \approx \begin{bmatrix} S_{11} \\ \vdots \\ S_{NN} \end{bmatrix} - \begin{bmatrix} d\Gamma_1^* \\ \vdots \\ d\Gamma_N^* \end{bmatrix} + (\mathbf{S} \circ \mathbf{S}^T) \cdot \begin{bmatrix} d\Gamma_1 \\ \vdots \\ d\Gamma_N \end{bmatrix} \quad (17)$$

where

$$\mathbf{S} \circ \mathbf{S}^T = \begin{bmatrix} S_{11}S_{11} & \cdots & S_{1N}S_{N1} \\ \vdots & \ddots & \vdots \\ S_{N1}S_{1N} & \cdots & S_{NN}S_{NN} \end{bmatrix}. \quad (18)$$

Here, \circ denotes the Hadamard (i.e., element-wise) product and the T superscript denotes transposition.

Embedding the rotation components of the various $d\Gamma_i$ into the network results in a modified scattering matrix $\tilde{\mathbf{S}}$. For such a configuration, (17) becomes

$$\begin{aligned} e^{j\Phi} \cdot \begin{bmatrix} dS_{11} \\ \vdots \\ dS_{NN} \end{bmatrix} &= e^{j\Phi} \cdot \left(\begin{bmatrix} S'_{11} \\ \vdots \\ S'_{NN} \end{bmatrix} - \begin{bmatrix} S_{11} \\ \vdots \\ S_{NN} \end{bmatrix} \right) \\ &\approx (\tilde{\mathbf{S}} \circ \tilde{\mathbf{S}}^T - \mathbf{1}) \cdot \begin{bmatrix} d\rho_1 \\ \vdots \\ d\rho_N \end{bmatrix} \end{aligned} \quad (19)$$

where

$$dS_{ij} = S'_{ij} - S_{ij} \quad (20)$$

$$\Phi = \begin{bmatrix} \phi_1 & & \\ & \ddots & \\ & & \phi_N \end{bmatrix} \quad (21)$$

$$\tilde{\mathbf{S}} = e^{j\Phi} \cdot \mathbf{S}. \quad (22)$$

Finally, rearranging yields

$$\begin{bmatrix} dS_{11} \\ \vdots \\ dS_{NN} \end{bmatrix} \approx e^{-j\Phi} \cdot (\tilde{\mathbf{S}} \circ \tilde{\mathbf{S}}^T - \mathbf{1}) \cdot \begin{bmatrix} d\rho_1 \\ \vdots \\ d\rho_N \end{bmatrix}. \quad (23)$$

Since $\tilde{\mathbf{S}}$ is strictly *g-us*, it satisfies (1). Therefore, by Gershgorin's circle theorem [14], the eigenvalues of $\tilde{\mathbf{S}} \circ \tilde{\mathbf{S}}^T - \mathbf{1}$ cannot vanish. Thus, $e^{-j\Phi} \cdot (\tilde{\mathbf{S}} \circ \tilde{\mathbf{S}}^T - \mathbf{1})$ is guaranteed to be invertible.

Consequently, perturbations $[d\rho_1 \ \dots \ d\rho_N]$ will always correspond to finite variations $[dS_{11} \ \dots \ dS_{NN}]^T$, and *vice versa*. Also, since the perturbations are realized through lossless matching networks, the overall scattering matrix will remain *g-us* (strictly) after any number of such perturbations as long as the port reflectances do not degenerate into reactive values. In turn, this degenerated behavior is prevented if the perturbations are guided toward lower reflectance magnitudes.

As a result of these properties, it is possible to control $[dS_{11} \ \dots \ dS_{NN}]^T$ through the choice of $[d\Gamma_1 \ \dots \ d\Gamma_N]^T$ and devise for it a path suitable for the attainment of the SCM condition, namely, by progressively reducing the magnitudes of the diagonal scattering parameters. Thus, the preceding discussion proves the main claim of this contribution, which is as follows.

*At f_0 , if \mathbf{S} is strictly *g-us*, then it is SCM-able to lossy terminations by cascading lossless two-ports to its ports.*

It is worth noting that the above derivation establishes the sought-for result by ensuring the existence of a path of perturbations which gradually transforms the original scattering matrix to a SCM-ed scattering matrix. The practical aspects of this, including the actual computation of the matching networks, are illustrated next in Section V.

V. "GUIDED" ALGORITHM (ALGG)

The discussion in Section IV does not only prove SCM-ability of *g-us* networks: it also serves as the basis for a numerical algorithm (ALGG) capable of realizing the SCM condition for those networks. In particular, expanding the complex-valued terms of (17) into real-valued terms and rearranging yields a linear problem of dimension $2N$ of the form

$$\begin{bmatrix} \text{Re}[\Delta S_{11}] \\ \text{Im}[\Delta S_{11}] \\ \vdots \\ \text{Re}[\Delta S_{NN}] \\ \text{Im}[\Delta S_{NN}] \end{bmatrix} = \mathbf{R} \cdot \begin{bmatrix} \text{Re}[\Delta \Gamma_1] \\ \text{Im}[\Delta \Gamma_1] \\ \vdots \\ \text{Re}[\Delta \Gamma_N] \\ \text{Im}[\Delta \Gamma_N] \end{bmatrix} \quad (24)$$

TABLE II

SCATTERING PARAMETERS OF THE NETWORK ANALYZED IN FIG. 3

$-0.3942 + 0.0356j$	$-0.2955 - 0.1378j$	$-0.1503 + 0.2054j$
$-0.1103 + 0.2873j$	$0.3640 - 0.3848j$	$-0.2612 + 0.5875j$
$0.2428 - 0.0124j$	$-0.1596 - 0.2642j$	$0.2359 + 0.3275j$

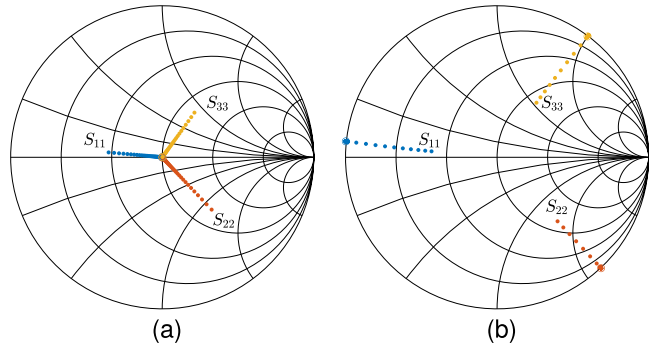


Fig. 3. Iterative matching of the scattering matrix in Table II. (a) $\epsilon = +0.1$. (b) $\epsilon = -0.1$.

where

$$\mathbf{R} = \begin{bmatrix} \mathbf{R}_{11} & \cdots & \mathbf{R}_{1N} \\ \vdots & \ddots & \vdots \\ \mathbf{R}_{N1} & \cdots & \mathbf{R}_{NN} \end{bmatrix} \quad (25)$$

$$\mathbf{R}_{ii} = \begin{bmatrix} \text{Re}[S_{ii}^2] - 1 & -\text{Im}[S_{ii}^2] \\ \text{Im}[S_{ii}^2] & \text{Re}[S_{ii}^2] + 1 \end{bmatrix} \quad (26)$$

$$\mathbf{R}_{ij} = \begin{bmatrix} \text{Re}[S_{ij}S_{ji}] & -\text{Im}[S_{ij}S_{ji}] \\ \text{Im}[S_{ij}S_{ji}] & \text{Re}[S_{ij}S_{ji}] \end{bmatrix}, \quad j \neq i. \quad (27)$$

Then, (24) is solved by inversion of \mathbf{R} (which is invertible because it just expresses in the real domain a perturbation which has been shown to be well defined in the complex domain). Specifically, the variations of the port reflectances, $\Delta S_{ii} = S'_{ii} - S_{ii}$, can be chosen such as to result in a magnitude reduction. For instance

$$S'_{ii} \stackrel{!}{=} (1 - \epsilon)S_{ii} \quad (28)$$

$$\Delta S_{ii} = -\epsilon S_{ii} \quad (29)$$

with ϵ some small, positive scalar. As an example, the scattering parameters given in Table II, which represent a *g-us* network, were subjected to the above algorithm, with $\epsilon = 0.1$. Fig. 3(a) shows the progressive reduction of the port reflectances, until the circuit is SCM-ed.

Since the matching actually improves at each iteration for this example, ϵ is left constant. However, should it happen that an iteration does not result in an improvement (as due to a step too large for the linearization to be valid), ϵ can be reduced until it does. Since by hypothesis we are considering *g-us* networks, we are guaranteed by the discussion in Section IV that, for sufficiently small $\epsilon \neq 0$, the linearization becomes valid.

Incidentally, Fig. 3(b) shows that the opposite behavior is obtained by choosing $\epsilon = -0.1$: in this case the diagonal

terms of the scattering matrix get arbitrarily close in magnitude to unity, forcing the off-diagonal elements to zero as a consequence of (1). In the limit, a diagonal matrix is obtained, which (consistently with the final remarks in Section III-B) is marginally *g-us*.

AlgG can be summarized formally as follows.

- 0) initialize $k = 1$.
- 1) Set ϵ equal to a small positive constant.
- 2) Compute ΔS_{ii} for all port numbers i according to (29).
- 3) Build matrix \mathbf{R} according to (25).
- 4) Compute $\Delta \Gamma_i$ for all i by inverting (24).
- 5) For all i , Compute a lossless matching network able to transform the origin into $\Delta \Gamma_i$ (Section III-A).
- 6) Cascade the matching networks at the relevant ports of \mathbf{S} , obtaining a new network \mathbf{S}' (Section III-B).
- 7) Increase k by one.
- 8) If k is over the maximum number of iterations or if $\max_i |S'_{ii}|$ is acceptable, stop.
- 9) If $|S'_{ii}| < |S_{ii}|$ for all i , replace $\mathbf{S} \leftarrow \mathbf{S}'$ and restart from step 1. Otherwise, replace $\epsilon \leftarrow \epsilon/2$ and restart from step 2.

It is worth noting that, at each iteration of step 5, a set of N lossless networks is computed, each of which is described by a 2×2 scattering matrix. Therefore, when the algorithm stops, an ordered sequence of k such matrices has been obtained for each port i . Cascading these matrices yields then an overall 2×2 matrix which represents a lossless matching network, and this operation can be repeated for all ports. The N lossless matching networks thus obtained realize the SCM condition for the original N -port.

VI. ALTERNATIVE APPROACHES

In order to prove the main claim of this contribution, i.e., that a *g-us* N -port network can be SCM-ed, Section IV above is sufficient. Similarly, Section V complements that theoretical finding with a practical implementation.

However, during their study of the problem at hand, the Authors have come across and investigated also different routes: the algorithms relevant to these alternative approaches are presented in Sections VI-A–VI-C as a basis for further research. In addition, it is worth discussing the straightforward approach of brute optimization. This has not been found helpful in showing the main claim nor has any inherent theoretical value; however, once the result is proven, circuit designers can most conveniently adopt this last approach.

A. “Single-Port” Algorithm (AlgS)

Consider the following iterative scheme (AlgS), which coincides with the algorithm proposed in [7] for matching antenna arrays.

- 0) Initialize $k = 1$.
- 1) Set $\iota = k \bmod N$; if $\iota \neq 0$, set $i = \iota$, otherwise set $i = N$.
- 2) Compute a lossless matching network able to conjugately match the S_{ii} parameter (Section III-A).
- 3) Cascade the matching network at the relevant port of \mathbf{S} , obtaining a new network \mathbf{S}' (Section III-B).

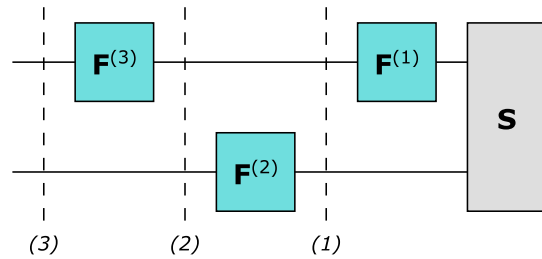


Fig. 4. Principle of the single-port iterative approach to SCM (AlgS), exemplified in the case $N = 2$.

- 4) Replace $\mathbf{S} \leftarrow \mathbf{S}'$.
- 5) Increase k by one.
- 6) If k is over the maximum number of iterations or if $\max_i |S'_{ii}|$ is acceptable, stop.
- 7) Restart from step 1.

Above, ι simply denotes a dummy index running cyclically over all port numbers. Fig. 4 offers a visualization of the proposed scheme in the two-port case.

It is easy to show that AlgS converges to the SCM condition in the case $N = 2$.

B. “All-Ports” Algorithm (AlgA)

Algorithm AlgA is described formally as follows.

- 0) Initialize $k = 1$.
- 1) For all i , compute a lossless matching network able to conjugately match the S_{ii} parameter (Section III-A).
- 2) For all i , cascade the matching networks at the relevant ports of \mathbf{S} , obtaining a new network \mathbf{S}' (Section III-B).
- 3) Replace $\mathbf{S} \leftarrow \mathbf{S}'$.
- 4) Increase k by one.
- 5) If k is over the maximum number of iterations or if $\max_i |S'_{ii}|$ is acceptable, stop.
- 6) restart from step 1.

Thus, it is apparent that AlgA resembles closely AlgS. However, instead of matching each port sequentially $(1, 2, \dots, N, 1, 2, \dots)$ as in algorithm AlgS, the AlgA scheme stipulates that all ports be cascaded, at each iteration, to their relevant matching networks. This corresponds to constructing a lossless $(2N)$ -port with scattering matrix \mathbf{H} as per Sections III-A and III-B with blocks given by

$$\mathbf{A} = \begin{bmatrix} -S_{11} & & & \\ & \ddots & & \\ & & & -S_{NN} \end{bmatrix} \quad (30)$$

$$\mathbf{B} = \mathbf{C} = \begin{bmatrix} \sqrt{1 - |S_{11}|^2} & & & \\ & \ddots & & \\ & & & \sqrt{1 - |S_{NN}|^2} \end{bmatrix} \quad (31)$$

$$\mathbf{D} = \begin{bmatrix} S_{11}^* & & & \\ & \ddots & & \\ & & & S_{NN}^* \end{bmatrix} \quad (32)$$

and terminating its last N ports in the circuit at hand. If the latter is represented at a given iteration by a scattering matrix \mathbf{S} ,

the updated matrix \mathbf{S}' is given by

$$\mathbf{S}' = \mathbf{A} + \mathbf{B}(\mathbf{S}^{-1} - \mathbf{D})^{-1}\mathbf{C} \quad (33)$$

$$= \mathbf{A} + \mathbf{B}\mathbf{S}\mathbf{C} + \mathbf{E} \quad (34)$$

$$\mathbf{E} = \mathbf{B} \left[\sum_{k=1}^{\infty} (\mathbf{S}\mathbf{D})^k \mathbf{S} \right] \mathbf{C} \approx \mathbf{S}\mathbf{D}\mathbf{S} \quad (35)$$

$$S'_{ii} = -S_{ii}|S_{ii}|^2 + E_{ii} \quad (36)$$

where the approximation in (35) holds for small S_{ii} terms. The AlgA iterative approach exhibits a construction similar to AlgG and is exemplified in Fig. 2 in the $N = 3$ case.

By exploiting (1), it is rather easy to prove the local convergence of this algorithm (i.e., convergence for a circuit whose S_{ii} parameters are sufficiently close to zero) for arbitrary N .

Notice that, as compared to AlgG and AlgS, AlgA can be applied in a user-independent, deterministic manner. Specifically, the evolution of the network parameters from each iteration to the next does not depend in any way on parameters set by the user (such as ϵ in AlgG) nor on the ordering of the ports (which is the case for AlgS). Thus, in case of convergence, it seems to express in a neater way the inherent characteristics of the network to which it is applied. For this reason, searching for a proof of global convergence of this algorithm is certainly worth further investigation.

C. Brute Optimization

As mentioned above, the merit of AlgG mainly lies in its validation of the claim in Section IV, i.e., the attainability of the SCM condition in g - us N -ports. However, once this property of g - us N -ports is proven, there is no actual need for using that algorithm rather than another, provided that the chosen alternative converges to the SCM condition. In particular, from the standpoint of a circuit designer, the most convenient way to achieve the SCM condition for a g - us N -port would be through brute optimization in an electronic software automation (EDA) environment. Notice that successful convergence is arguably very likely but not guaranteed mathematically. At any rate, multiple optimization runs with different starting values could be tried in the remote possibility that convergence is not achieved right away.

A very straightforward way to attain the SCM condition for a given g - us N -port through optimization is based on the usage of matching networks such as those shown in Fig. 5. These are designed to be lossless by construction and, at the same time, are sufficiently general that they can be equivalent to any possible lossless two-port at the considered frequency. As to the optimization algorithm itself, to be used to determine the values of the components in the matching networks, there are plenty of these. However, gradient-based algorithms are an efficient choice. For these, it is possible to show local convergence (as for AlgA in Section VI-B), whereas a proof of global convergence is not available.

VII. APPLICATION EXAMPLES

In Sections VII-A–VII-D, several examples of application of the presented theory are proposed. The first one, represented by a spiral Marchand balun, is worked out in full so as to

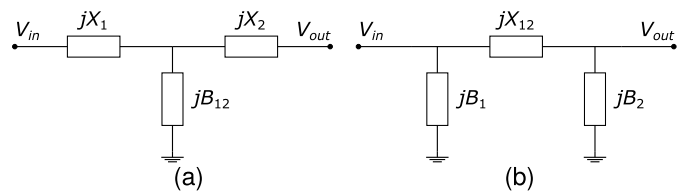


Fig. 5. Three-element lossless matching networks in (a) T and (b) Π topology.

TABLE III
SCATTERING PARAMETERS OF THE SPIRAL MARCHAND
BALUN ANALYZED IN SECTION VII-A

$-0.4223 - 0.6087j$	$0.2026 + 0.3688j$	$-0.1309 - 0.2664j$
$0.2026 + 0.3688j$	$0.0977 + 0.7800j$	$-0.0992 + 0.0964j$
$-0.1309 - 0.2664j$	$-0.0992 + 0.0964j$	$0.0987 + 0.8313j$

TABLE IV
SCATTERING PARAMETERS OF THE SPIRAL MARCHAND BALUN
ANALYZED IN SECTION VII-A AFTER EMBEDDING
THE MATCHING NETWORKS

$0.0000 + 0.0000j$	$0.4454 + 0.4441j$	$-0.2823 - 0.3217j$
$0.4454 + 0.4441j$	$0.0000 + 0.0000j$	$-0.0765 + 0.3221j$
$-0.2823 - 0.3217j$	$-0.0765 + 0.3221j$	$0.0000 + 0.0000j$

TABLE V
SCATTERING PARAMETERS OF THE MATCHING NETWORKS COMPUTED
FOR THE SPIRAL MARCHAND BALUN IN SECTION VII-A

MN1	$-0.0614 + 0.5010j$	$0.8629 + 0.0246j$
	$0.8629 + 0.0246j$	$0.0328 + 0.5037j$
MN2	$0.1328 - 0.7825j$	$0.6070 + 0.0390j$
	$0.6070 + 0.0390j$	$-0.0315 - 0.7931j$
MN3	$0.0408 - 0.8413j$	$0.5384 + 0.0243j$
	$0.5384 + 0.0243j$	$0.0350 - 0.8416j$

allow the interested Readers to replicate it. For this example, in particular, we report the scattering matrices of the original network (Table III), of the SCM-ed network as computed by AlgG (Table IV) and of the three matching networks resulting as a by-product of AlgG (Table V), as well as a list of all possible T- and Π -topology realizations with ideal elements. In addition, we design the matching networks with realistic models of these elements and provide the scattering matrix of the final design ready for realization (Table VI). This is to show that, whereas AlgG yields a perfectly SCM-ed scattering matrix, imperfect matching is unavoidable in practice due to the nonideal behavior of the available components. A remarkably good agreement between simulations and measurements is found for both the original and matched networks. To ease the reading, the simulations and measurements are split between Sections VII-A and VII-B, respectively.

TABLE VI
SCATTERING PARAMETERS OF THE SPIRAL MARCHAND BALUN
ANALYZED IN SECTION VII-A AT LAYOUT STAGE

$-0.2953 + 0.1165j$	$-0.4213 - 0.2389j$	$0.3014 + 0.1576j$
$-0.4213 - 0.2389j$	$0.0563 + 0.0056j$	$-0.0943 + 0.3343j$
$0.3014 + 0.1576j$	$-0.0943 + 0.3343j$	$0.0975 + 0.0236j$

The remaining examples are presented with a lower level of detail, with the primary goal of demonstrating specific claims. Section VII-C starts with illustrating through simulations the case of a ten-element array. As expected, no difficulty is incurred as a consequence of the comparatively large value of N . The remainder of the section deals with a simpler design where N is decreased to 3, in order to lead to measurable test vehicles. Also in this case measurements confirm the correctness of the design.

The final example, in Section VII-D, involves a paraphase amplifier and is chosen to show that, as per theory, active networks do not entail any particular problems: as long as these are g - us at the frequency at which the SCM condition has to be realized, the execution of AlgG is not affected.

A. Spiral Marchand Balun: Simulations

In the following, the proposed theory is applied to a realistic circuit, i.e., a spiral Marchand balun designed in process PIH1–10 by WIN Semiconductors for operation at 15 GHz, shown in Fig. 6. At the lower frequency $f_0 = 5$ GHz, the scattering parameters of the balun, given in Table III, are mismatched and exhibit an amplitude imbalance of approximately 3 dB. These data represent the starting point for application of the AlgG at f_0 , as per Section V.

Applying AlgG produces, first of all, the scattering matrix of a matched balun, as per Table IV. As a by-product, it is possible to compute at each port the parameters of an overall lossless matching network by cascading the partial matching networks relevant to all iterations: see final comments of Section V. The obtained parameters are reported in Table V.

Each of these matching networks is by construction a lossless two-port and, therefore, can be realized in T or Π topology by exploiting the formulas in [15]. Specifically, the first matching network can be implemented in any of the following forms.

- 1) $L_{1,s} = 0.267511$ nH, $L_{2,p} = 2.587290$ nH, $L_{3,s} = 0.549777$ nH.
- 2) $L_{1,s} = 5.442080$ nH, $C_{2,p} = 0.391612$ pF, $L_{3,s} = 5.724350$ nH.
- 3) $L_{1,p} = 4.11372$ nH, $L_{2,s} = 0.874132$ nH, $L_{3,p} = 8.454330$ nH.
- 4) $L_{1,p} = 0.395090$ nH, $C_{2,s} = 1.159110$ pF, $L_{3,p} = 0.415582$ nH.

Here the p and s subscripts denote, respectively, a shunt or a series element. Similarly for the second matching network.

- 1) $C_{1,s} = 0.273435$ pF, $L_{2,p} = 1.334850$ nH, $C_{3,s} = 0.302989$ pF.

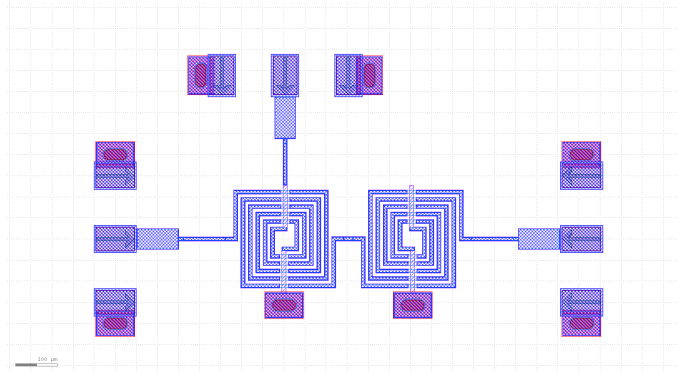


Fig. 6. Spiral Marchand balun analyzed in Section VII. Ports are numbered progressively from the top one in a clockwise fashion. Approximate chip size: $1200 \times 700 \mu\text{m}^2$.

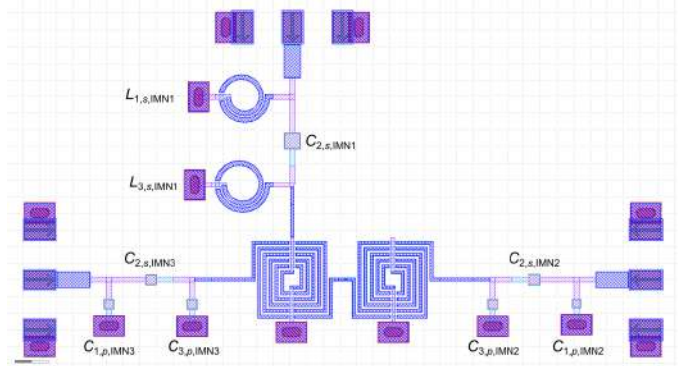


Fig. 7. Spiral Marchand balun of Section VII-A with the addition of the matching networks. Ports are numbered progressively from the top one in a clockwise fashion. Approximate chip size: $1950 \times 1050 \mu\text{m}^2$.

- 2) $C_{1,s} = 0.978207$ pF, $C_{2,p} = 0.759044$ pF, $C_{3,s} = 1.502510$ pF.
- 3) $C_{1,p} = 1.136510$ pF, $L_{2,s} = 2.233390$ nH, $C_{3,p} = 1.259350$ pF.
- 4) $C_{1,p} = 0.229184$ pF, $C_{2,s} = 0.453665$ pF, $C_{3,p} = 0.352023$ pF.

The third.

- 1) $C_{1,s} = 0.329393$ pF, $L_{2,p} = 1.075960$ nH, $C_{3,s} = 0.330646$ pF.
- 2) $C_{1,s} = 1.096460$ pF, $C_{2,p} = 0.941681$ pF, $C_{3,s} = 1.110460$ pF.
- 3) $C_{1,p} = 1.101340$ pF, $L_{2,s} = 2.620120$ nH, $C_{3,p} = 1.105520$ pF.
- 4) $C_{1,p} = 0.327928$ pF, $C_{2,s} = 0.386704$ pF, $C_{3,p} = 0.332116$ pF.

In the present case, the matching networks at each port have been implemented in the fourth form presented.

Up to this point, the presented data are either an input (the original balun) or the result of assuming ideal components (in the matching networks): therefore, these data can be used by the interested Reader to replicate the proposed approach.

For completeness, however, the performance of the final circuit at layout stage is also reported. Of course, the perfect behavior obtained in Table IV deteriorates when the ideal elements are replaced by real ones, which are affected by parasitic effects. The EM-simulated scattering parameters of the final circuit, depicted in Fig. 7, are shown in Table VI at f_0 .

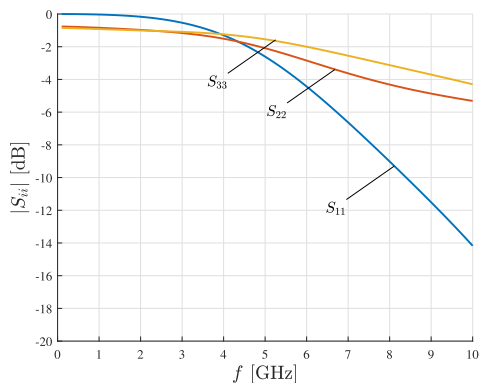


Fig. 8. Simulated port matching of the spiral Marchand balun analyzed in Section VII-A.

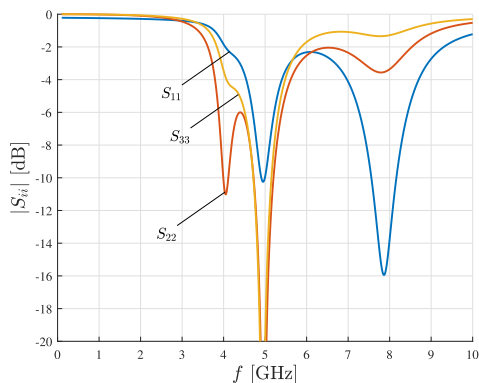


Fig. 9. Simulated port matching of the spiral Marchand balun analyzed in Section VII-A with the addition of the matching networks.

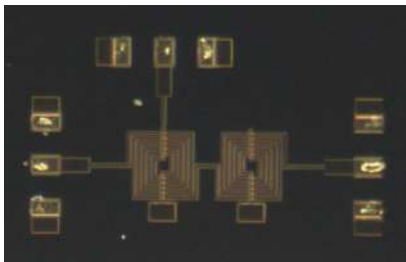


Fig. 10. Spiral Marchand balun analyzed in Section VII. Ports are numbered progressively from the top one in a clockwise fashion. Approximate chip size: $1200 \times 700 \mu\text{m}^2$.

The reflectances over frequency of the original and matched circuits are shown in Figs. 8 and 9, respectively.

B. Spiral Marchand Balun: Measurements

The Marchand balun discussed in Section VII-A has been fabricated in both its original and matched versions. Pictures of the two circuits are presented in Figs. 10 and 11, respectively.

Since the circuits are three-port networks, measuring them as such is not straightforward. In this case, the test vehicles have been measured after two different calibrations: one with VNA ports aligned, the other with ports at 90° . The full set of scattering parameters is thus retrieved. Actually, a residual error arises from the fact that, for each configuration, the DUT port not connected to the VNA is terminated in an imperfect load, but this effect is negligible here.

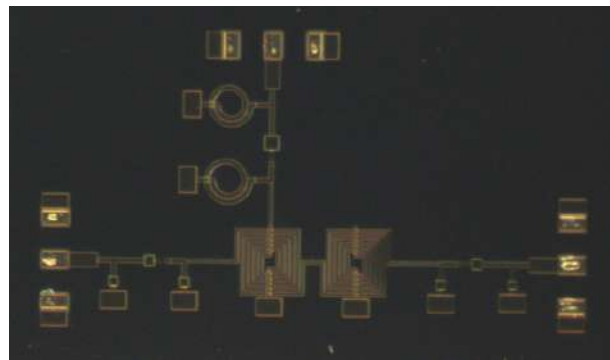


Fig. 11. Spiral Marchand balun analyzed in Section VII-A with the addition of the matching networks. Ports are numbered progressively from the top one in a clockwise fashion. Approximate chip size: $1950 \times 1050 \mu\text{m}^2$.

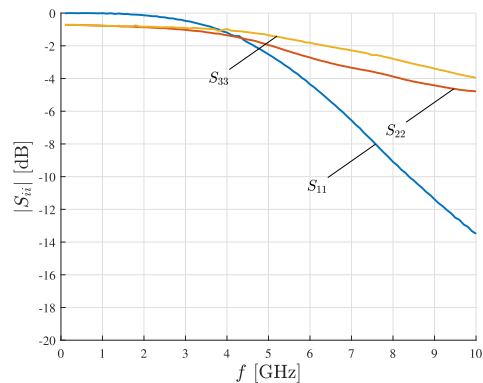


Fig. 12. Measured port matching of the spiral Marchand balun analyzed in Section VII-A.

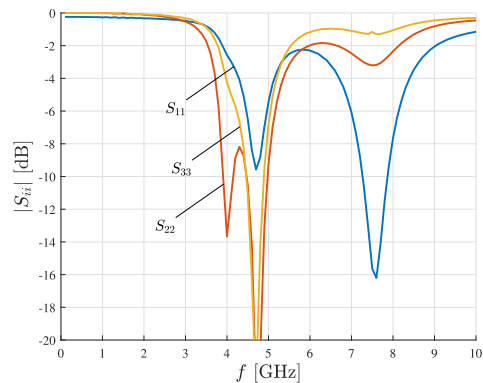


Fig. 13. Measured port matching of the spiral Marchand balun analyzed in Section VII-A with the addition of the matching networks.

The measured reflectances of the original and matched baluns are shown in Figs. 12 and 13, respectively. Except for a slight frequency detuning in the matched version, measurements are in good agreement with the simulations.

C. Antenna Array

As mentioned above, antenna arrays represent a case of N -port networks for which N can be arbitrarily large. However, thanks to passivity, they are inherently *us*: therefore, they can always be SCM-ed at any given frequency, irrespective of N . As an example, a ten-element array of patches is designed for operation at 100 GHz on WIN Semiconductors'

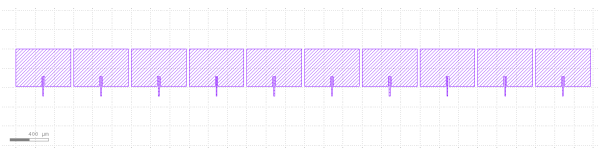


Fig. 14. Layout of a ten-element antenna array analyzed in Section VII-C. Ports are numbered progressively from the leftmost one toward the right. Approximate chip size: $6000 \times 500 \mu\text{m}^2$.

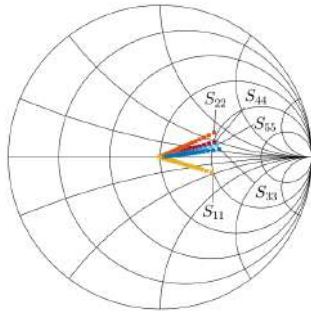


Fig. 15. Iterative matching of the ten-element antenna array analyzed in Section VII-C. Ports from 6 to 10 behave identically to ports from 5 to 1 due to symmetry.

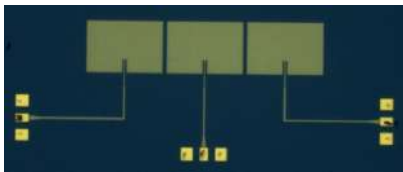


Fig. 16. Microphoto of the three-element antenna array analyzed in Section VII-C. Ports are numbered progressively from the left-hand one in a clockwise fashion. Approximate chip size: $2900 \times 1100 \mu\text{m}^2$.

PP10–20 100-nm GaAs pHEMT process. The array layout is shown in Fig. 14. AlgG is applied without difficulty to the resulting 10×10 scattering matrix, resulting in the progressive improvement of the S_{ii} parameter for all i until the SCM condition is reached, as shown in Fig. 15.

On the one hand, the above shows that large N values do not entail any issue in running AlgG. On the other hand, obvious difficulties would arise when trying to realize and measure a ten-port circuit. Thus, a simpler test vehicle is finalized for the purposes of the present illustration, namely, a three-element array, as shown in Fig. 16. The EM simulation at 100 GHz predicts a coupling between each pair of patches of approximately -7.7 dB, and a maximum array gain of 3.5 dB in the broadside direction with in-phase excitations.

Applying AlgG yields the scattering parameters of the matching networks, which in this case are realized through distributed elements due to the high frequency of operation. The end result is depicted in Fig. 17. Measured driving-point scattering parameters before and after adding the matching networks are reported in Figs. 18 and 19, respectively. It is evident that, whereas the bare array exhibits a bad return loss at port-3 at 100 GHz, the version including the matching networks is SCM-ed.

D. Paraphase Amplifier

As a last example, a paraphase amplifier is selected, realized on WIN Semiconductors' PP10–20 100-nm GaAs

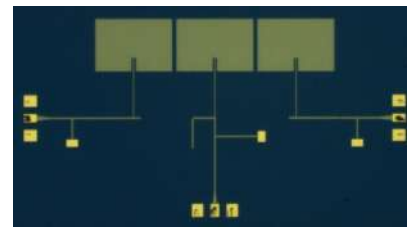


Fig. 17. Microphoto of the three-element antenna array analyzed in Section VII-C with the addition of the matching networks. Ports are numbered progressively from the left-hand one in a clockwise fashion. Approximate chip size: $2900 \times 1500 \mu\text{m}^2$.

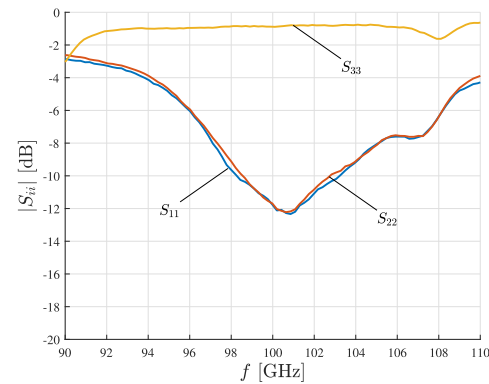


Fig. 18. Measured port matching of the three-element antenna array analyzed in Section VII-C.

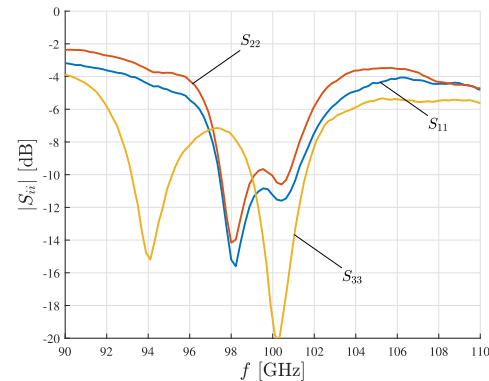


Fig. 19. Measured port matching of the three-element antenna array analyzed in Section VII-C with the addition of the matching networks.

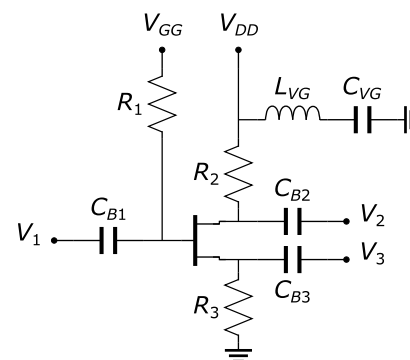


Fig. 20. Circuit schematic of the paraphase amplifier analyzed in Section VII-D.

pHEMT process. The circuit schematic and a microphoto of the amplifier, which has already been discussed in [16], are reproduced in Figs. 20 and 21, respectively. As opposed to the

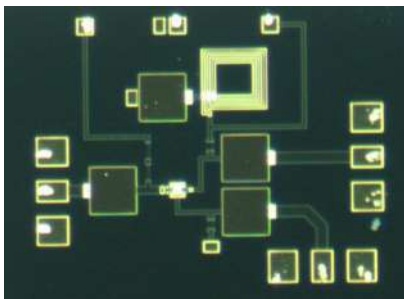


Fig. 21. Microphoto of the paraphase amplifier analyzed in Section VII-D. The upper pads are for gate bias and drain supply. The left pads are for the input signal, whereas the right and bottom pads are for the two outputs. The three RF ports are numbered progressively from the left-hand one in a clockwise fashion. Approximate chip size: $1.2 \times 0.9 \text{ mm}^2$.

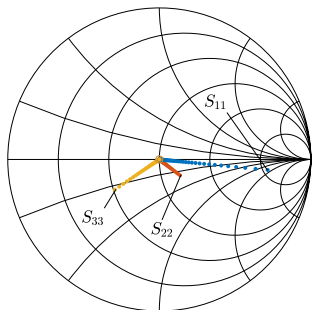


Fig. 22. Iterative matching of the paraphase amplifier analyzed in Section VII-D.

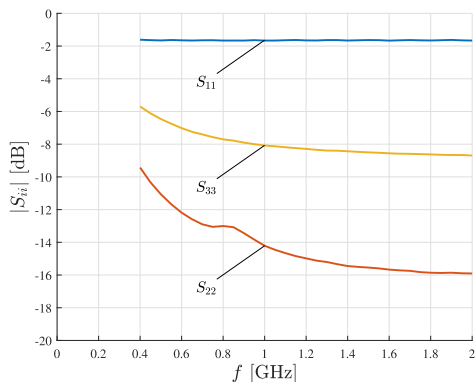


Fig. 23. Measured port matching of the spiral paraphase amplifier analyzed in Section VII-D.

previous circuits, this one is active and, as such, requires that its unconditional stability be checked in order to guarantee a priori that AlgG will converge. However, this check has already been carried out in [16], which also reports measured scattering parameters of the paraphase amplifier. The next step is then applying AlgG, which as expected converges to the SCM without difficulty: the relevant iterations are shown in Fig. 22. The measured port reflectances of the amplifier alone and those simulated after applying the matching networks, are shown in Fig. 23 and Fig. 24, respectively.

The nominal gain at 1 GHz of both paths is -2.3 dB , as predicted from simulations and confirmed by measurements. The simulated gain after adding the matching networks is -0.5 dB .

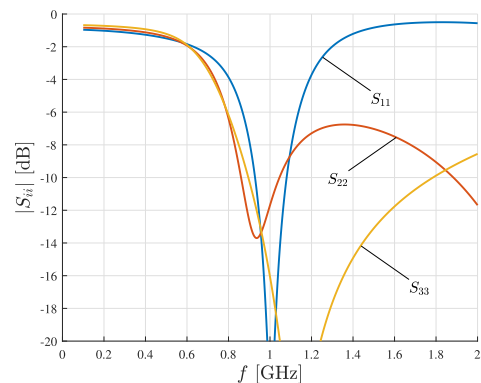


Fig. 24. Simulated port matching of the spiral paraphase amplifier analyzed in Section VII-D with the addition of the matching networks.

VIII. CONCLUSION

In this contribution, it has been shown that SCM can always be obtained for *g-us* N -ports. The proof is readily translated into an explicit algorithm (AlgG) which, by way of guided iterations, is mathematically guaranteed to converge to the SCM condition. The external reference impedance is assumed passive and the matching networks lossless.

As minor results, two more algorithms (AlgS and AlgA) have been presented which are believed by the Authors to always reach the SCM condition. For the time being, however, global convergence of AlgS could only be proven in the 2-port case, whereas AlgA has been proven to converge with arbitrary N but only locally.

The presented theory has been successfully applied to a numerous set of realistic circuits, namely, a spiral Marchand balun, a couple of antenna arrays and a paraphase amplifier. While the first example has been worked out in full to allow the interested Readers to replicate the presented results, the others are presented with lower detail to show that no difficulties arise when considering large values of N or active networks (as long as the latter are *g-us*).

APPENDIX

SCM IN TWO-PORT NETWORKS

Given a two-port network with scattering matrix \mathbf{S} , the source and load reflection coefficients satisfying the SCM condition can be computed in closed form [4], [17], [18]

$$\Gamma_{L,i,\text{conj}} = \frac{B_i \pm \sqrt{B_i^2 - 4|C_i|^2}}{2C_i} \quad (37)$$

$$B_i = 1 + |S_{ii}|^2 - |S_{jj}|^2 - |\Delta|^2 \quad (38)$$

$$C_i = S_{ii} - \Delta \cdot S_{jj}^* \quad (39)$$

$$\Delta = \det(\mathbf{S}) \quad (40)$$

$$\Gamma_{L,j,\text{conj}} = m_{ji}(\Gamma_{L,i,\text{conj}})^* \quad (41)$$

$$m_{ji}(\Gamma_{L,i}) = S_{jj} + \frac{S_{ij}S_{ji}\Gamma_{L,i}}{1 - S_{ii}\Gamma_{L,i}} \quad (42)$$

where $(i = 1, j = 2)$ or $(i = 2, j = 1)$, with $|\Gamma_{L,i,\text{conj},-} \cdot \Gamma_{L,i,\text{conj},+}| = 1$ by construction. Notice, in particular, that once $\Gamma_{L,i,\text{conj}}$ has been determined as one of the solutions of (37), $\Gamma_{L,j,\text{conj}}$ follows unambiguously through (41).

Alternatively, $\Gamma_{L,j,\text{conj}}$ can be computed directly through (37) by exchanging i and j . In fact, this is the usual procedure. In this respect, it is regarded as a matter of fact [4], [17], [18] that the sign determinations should be the same for $\Gamma_{L,i,\text{conj}}$ and $\Gamma_{L,j,\text{conj}}$ in order to get corresponding terminations. *However, to the best of the Authors' knowledge, such a result is not obvious and has not been demonstrated in the literature except for the trivial case of g-US [18].*

In the following, it will be shown through geometrical arguments that the usual sign determination is actually correct when $|K| > 1$, K being Rollett's stability factor [1], [2], and that the SCM condition can be realized with passive terminations if and only if the two-port satisfies $K > 1$. The findings and terminology from [19] and [20] will be exploited. Also, recall from [2] that $K > 1 \implies B_i B_j > 0$ and notice that, by the same argument, it is easily shown that $K < -1 \implies B_i B_j < 0$.

A. $|K| \leq 1$

This condition is equivalent to $|B_i| \leq 2|C_i|$, as per [4], [17], [18], [21], [22]. Thus, both $\Gamma_{L,i,\text{conj},+}$ and $\Gamma_{L,i,\text{conj},-}$ are purely reactive rather than strictly passive. Therefore, the SCM condition cannot be achieved on strictly passive terminations.

In all other cases (i.e., $|K| > 1$) either $\Gamma_{L,i,\text{conj},+}$ or $\Gamma_{L,i,\text{conj},-}$ will be strictly passive and the other strictly active, depending on the sign of B_i .

B. $K > 1$, $B_i > 0$, $B_j > 0$

These conditions describe a *g-us* two-port. Thus, the passive determination, $\Gamma_{L,i,\text{conj},-}$, will be mapped to a passive reflectance at port j by $m_{ji}(\cdot)$. Since $\Gamma_{L,i,\text{conj},-}$ satisfies the SCM conditions by construction, $m_{ji}(\Gamma_{L,i,\text{conj},-})^*$ has to be equal to either $\Gamma_{L,j,\text{conj},+}$ or $\Gamma_{L,j,\text{conj},-}$: it follows that the latter is the correct one, since it is passive too. By exclusion, the other pair of mutually associated terminations is composed of $\Gamma_{L,i,\text{conj},+}$ and $\Gamma_{L,j,\text{conj},+}$.

C. $K > 1$, $B_i < 0$, $B_j < 0$

These conditions describe a specific type of conditionally *g-us* two-port, i.e., one which satisfies the IRUS* and ORUS* configurations [19], [20]. Since at either section one determination expresses a passive and an active termination which, within a conjugation, map to an analogous pair at the other section, we must have (unsurprisingly) that one termination lies within the relevant stability region, and the other outside of it. As per the IRUS* and ORUS* configurations, the stability circles will be inside the unit disk and the stable region will be the internal one. Thus, the passive determination, $\Gamma_{L,i,\text{conj},+}$, will also have to lie in the stable region, i.e., inside the stability circle. Therefore $\Gamma_{L,i,\text{conj},+}$ is associated with $\Gamma_{L,j,\text{conj},+}$, which is also passive. By exclusion, $\Gamma_{L,i,\text{conj},-}$ and $\Gamma_{L,j,\text{conj},-}$ are associated with each other.

D. $K < -1$, $B_i > 0$, $B_j < 0$

If ($i = 1$, $j = 2$), these conditions describe a two-port satisfying IRUS and OUS* whereas, if ($i = 2$, $j = 1$), IUS*

and ORUS will hold [19], [20]. In general, the unstable region at port j will encompass the whole unit disk. Therefore the passive determination $\Gamma_{L,j,\text{conj},+}$ will be associated with the active determination $\Gamma_{L,i,\text{conj},+}$. By exclusion, the other pair is composed of $\Gamma_{L,j,\text{conj},-}$ and $\Gamma_{L,i,\text{conj},-}$, so that also in this case the signs match with each other. However, unlike the other cases where $|K| > 1$, here we are getting solution pairs where only one of the terminations is passive, while the other is active. Therefore, in this case the SCM condition cannot be achieved on passive terminations.

ACKNOWLEDGMENT

The authors would like to thank WIN Semiconductors, which supplied the technology to the Microwave Engineering Center for Space Applications (MECSA) in the framework of the initiative "mmWave Multi-Project Runs For Select Universities."

REFERENCES

- [1] J. Rollett, "Stability and power-gain invariants of linear twoports," *IRE Trans. Circuit Theory*, vol. 9, no. 1, pp. 29–32, Mar. 1962.
- [2] D. Woods, "Reappraisal of the unconditional stability criteria for active 2-port networks in terms of S parameters," *IEEE Trans. Circuits Syst.*, vol. CAS-23, no. 2, pp. 73–81, Feb. 1976.
- [3] A. L. Hieber and R. J. Vernon, "Matching considerations of lossless reciprocal 5-port waveguide junctions (short papers)," *IEEE Trans. Microw. Theory Techn.*, vol. MTT-21, no. 8, pp. 547–552, Aug. 1973.
- [4] D. M. Pozar, *Microwave Engineering*, 4th ed. Hoboken, NJ, USA: Wiley, 2012.
- [5] S. Colangeli, W. Ciccognani, A. Serino, P. E. Longhi, and E. Limiti, "A bound on the scattering parameters of unconditionally stable N-ports," *IEEE Trans. Circuits Syst. II, Exp. Briefs*, vol. 70, no. 3, pp. 855–859, Mar. 2023.
- [6] S. Colangeli, W. Ciccognani, A. Serino, P. E. Longhi, and E. Limiti, "The stability radius: A new indicator of unconditional stability for N-Port linear networks," *IEEE Microw. Wireless Compon. Lett.*, vol. 32, no. 9, pp. 1023–1026, Sep. 2022.
- [7] K. Kaga, K. Li, K. Honda, and K. Ogawa, "A sequential automatic impedance-matching algorithm to achieve simultaneous complex-conjugate condition in multi-element antennas," in *Proc. IEEE Int. Workshop Electromagn. (iWEM)*, Aug. 2014, pp. 24–25.
- [8] H. W. Bode, *Network Analysis and Feedback Amplifier Design*. New York, NY, USA: D. Van Nostrand Co. Inc., 1945.
- [9] K. Kurokawa, "Power waves and the scattering matrix," *IEEE Trans. Microw. Theory Techn.*, vol. MTT-13, no. 2, pp. 194–202, Mar. 1965.
- [10] S. Colangeli, W. Ciccognani, P. E. Longhi, and E. Limiti, "A test for unconditional stability based on polynomial convexification," *IEEE Trans. Microw. Theory Techn.*, vol. 68, no. 10, pp. 4177–4187, Oct. 2020.
- [11] S. Colangeli, W. Ciccognani, and E. Limiti, "Algorithmic test of the unconditional stability of three-port networks," *IEEE Trans. Microw. Theory Techn.*, vol. 66, no. 12, pp. 5197–5205, Dec. 2018.
- [12] S. Colangeli, R. Cleriti, D. Palombini, and E. Limiti, "On the unconditional stability of N-port networks," in *Proc. 44th Eur. Microw. Conf.*, Oct. 2014, pp. 1520–1523.
- [13] M. Ohtomo, "Stability analysis and numerical simulation of multidevice amplifiers," *IEEE Trans. Microw. Theory Techn.*, vol. 41, no. 6, pp. 983–991, Jun. 1993.
- [14] E. Bodewig, *Matrix Calculus*. Amsterdam, The Netherlands: Elsevier, 1959.
- [15] W. Ciccognani, S. Colangeli, E. Limiti, and P. Longhi, "Noise measure-based design methodology for simultaneously matched multi-stage low-noise amplifiers," *IET Circuits, Devices Syst.*, vol. 6, no. 1, p. 63, 2012.
- [16] S. Colangeli, A. Serino, W. Ciccognani, P. E. Longhi, and E. Limiti, "Additional findings on S-parameter bounds valid for unconditionally stable N-ports," *Int. J. Numer. Modelling: Electron. Netw., Devices Fields*, vol. 37, no. 2, Mar. 2024.
- [17] G. Gonzalez, *Microwave Transistor Amplifiers: Analysis and Design*, 2nd ed. Upper Saddle River, NJ, USA: Prentice-Hall, 1996.

- [18] R. E. Collin, *Foundations for Microwave Engineering* (IEEE Press Series on Electromagnetic Wave Theory), 2nd ed., D. J. Dudley, Ed. Hoboken, NJ, USA: Wiley, 1992.
- [19] G. Lombardi and B. Neri, "On the relationships between input and output stability in two-ports," *IEEE Trans. Circuits Syst. I, Reg. Papers*, vol. 66, no. 7, pp. 2489–2495, Jul. 2019.
- [20] G. Lombardi and B. Neri, "Microwave circuit conditional stability: Two-parameter criteria," *IEEE Trans. Circuits Syst. II, Exp. Briefs*, vol. 67, no. 12, pp. 2913–2917, Dec. 2020.
- [21] A. Serino, W. Ciccognani, S. Colangeli, P. E. Longhi, and E. Limiti, "New proofs of the two-port networks unconditional stability criteria based on the rollett k parameter," *IEEE Trans. Circuits Syst. I, Reg. Papers*, vol. 69, no. 4, pp. 1441–1451, Apr. 2022.
- [22] M. L. Edwards, S. Cheng, and J. H. Sinsky, "A deterministic approach for designing conditionally stable amplifiers," *IEEE Trans. Microw. Theory Techn.*, vol. 43, no. 7, pp. 1567–1575, Jul. 1995.

Sergio Colangeli was born in Rome, Italy, in 1984. He received the Ph.D. degree in telecommunications and microelectronics from the University of Rome Tor Vergata, Rome, in 2013.

He has been with the Department of Electronics, University of Rome Tor Vergata, where he is currently as an Associate Professor. His research interests include low-noise design methodologies for microwave applications, with particular reference to low-noise amplification, small-signal and noise characterization and modeling of microwave active devices, and stability analysis of linear and nonlinear circuits.

Dr. Colangeli was a recipient of the EuMIC Young Engineer Prize in 2012.

Antonio Serino received the M.S. degree in electronic engineering from the University of Rome Tor Vergata, Rome, Italy, in 1994.

From 1998 to 2000, he worked as a Graduate Technician with the University of Rome Tor Vergata, where he became an Assistant Professor in 2001. His research interests include small-signal and large-signal characterization and modeling of microwave and millimeter wave active devices, noise characterization and modeling of field effect transistors for microwave and millimeter wave applications, and design methodologies of millimeter wave low noise amplifiers.

Walter Ciccognani was born in Rome, Italy, in 1977. He received the M.S. degree in electronic engineering and the Ph.D. degree in telecommunications and microelectronics from the University of Rome Tor Vergata, Rome, in 2002 and 2007, respectively.

He has been an Assistant Professor since 2012, University of Rome Tor Vergata, and where he has been teaching the course in microwave measurements since 2013. He has coauthored over 60 papers in international scientific journals and conferences and has been involved in several national and international research projects, and in those contexts he had the opportunity to collaborate with the major European semiconductor foundries. His main interests include linear microwave circuit-design methodologies, linear and noise analysis/measurement techniques, and small-signal and noise modeling of microwave active devices.

Patrick E. Longhi (Member, IEEE) received the M.S. degree in electronic engineering and the Ph.D. degree in microelectronics from the University of Rome Tor Vergata, Rome, Italy, in 2004 and 2009, respectively.

From 2009 to 2018, he was at ELT-Elettronica SpA, Rome, holding different managerial and technical positions in Engineering, Manufacturing, and Sales. Since August 2018, he has been an Assistant Professor with the Department of Electronic Engineering, University of Rome Tor Vergata. His main fields of interests include the design of microwave and millimeter-wave LNAs, RF amplitude control circuits (variable gain amplifiers and attenuators), and mixers.

Ernesto Limiti (Senior Member, IEEE) was a Research and Teaching Assistant (1991–1997), an Associate Professor (1998–2001), and since has been a Full Professor of electronics with the Department of EE, University of Rome Tor Vergata, Rome, Italy.

He has authored or coauthored over 350 publications on refereed international journals and presentations within international conferences. He is a referee of the international journals of the microwave and millimeter-wave electronics sector. His research activity is focused on three main lines, all of them belonging to the microwave and millimeter-wave electronics area. The first one is related to characterization and modeling for active and passive microwave and millimeter-wave devices. Regarding active devices, the research line is oriented to small-signal, noise, and large-signal modeling. For active devices, novel methodologies have been developed for the noise characterization and the subsequent modeling, and equivalent-circuit modeling strategies have been implemented both for small- and large-signal operating regimes for GaAs, GaN, SiC, Si, and InP MESFET/HEMT devices. The second line is related to design methodologies and characterization methods for low-noise devices and circuits. The main focus is on cryogenic amplifiers and devices. Finally, the third line is in the analysis and design methodologies for linear and nonlinear microwave circuits.

Prof. Limiti is a member of the Steering Committee of international conferences and workshops. He has been the President of the Laurea and the Laurea Magistrale degrees in electronic engineering, University of Rome Tor Vergata, and a member of the Committee of the Ph.D. Program in telecommunications and microelectronics, tutoring an average of four doctoral candidates per year.